

Journal of Biomedical Optics

BiomedicalOptics.SPIEDigitalLibrary.org

Pulse transit time differential measurement by fiber Bragg grating pulse recorder

Sharath Umesh
Srivani Padma
Shikha Ambastha
Anand Kalegowda
Sundarrajan Asokan

Pulse transit time differential measurement by fiber Bragg grating pulse recorder

Sharath Umesh,^a Srivani Padma,^{a,b} Shikha Ambastha,^a Anand Kalegowda,^c and Sundarrajan Asokan^{a,d,*}

^aIndian Institute of Science, Department of Instrumentation and Applied Physics, Bangalore, India

^bIndian Institute of Science, Department of Electrical Communication Engineering, Bangalore, India

^cM.S. Ramaiah Medical College, Department of Radio Diagnosis, Bangalore, India

^dIndian Institute of Science, Robert Bosch Center for Cyber Physical Systems and Applied Photonics Initiative, Bangalore, India

Abstract. The present study reports a noninvasive technique for the measurement of the pulse transit time differential (PTTD) from the pulse pressure waveforms obtained at the carotid artery and radial artery using fiber Bragg grating pulse recorders (FBGPR). PTTD is defined as the time difference between the arrivals of a pulse pressure waveform at the carotid and radial arterial sites. The PTTD is investigated as an indicator of variation in the systolic blood pressure. The results are validated against blood pressure variation obtained from a Mindray Patient Monitor. Furthermore, the pulse wave velocity computed from the obtained PTTD is compared with the pulse wave velocity obtained from the color Doppler ultrasound system and is found to be in good agreement. The major advantage of the PTTD measurement via FBGPRs is that the data acquisition system employed can simultaneously acquire pulse pressure waveforms from both FBGPRs placed at carotid and radial arterial sites with a single time scale, which eliminates time synchronization complexity. © 2015 Society of Photo-Optical Instrumentation Engineers (SPIE) [DOI: 10.1117/1.JBO.20.5.057005]

Keyword: fiber Bragg grating pulse recorder; pulse transit time differential; pulse wave velocity; variation in systolic blood pressure monitoring.

Paper 150065R received Feb. 4, 2015; accepted for publication Apr. 30, 2015; published online May 28, 2015.

1 Introduction

Hypertension is known to adversely affect the cardiovascular and renal systems.¹ Precise blood pressure measurement is imperative as it can aid in the prognosis of hypertension and cardiovascular morbidity. The clinical usage of direct intra-arterial measurement of blood pressure is limited² due to its invasive nature.³ Conventional methods of blood pressure measurement utilize auscultatory or oscillometric techniques, which are cuff based methods with various disadvantages, prominent being the inability to continuously measure beat-to-beat blood pressure. Further, these techniques necessitate 1 to 2 min time duration between consecutive blood pressure measurements.⁴ Other methods such as tonometry, finger-cuff method, and ultrasound techniques are able to provide beat-to-beat blood pressure; however, they are limited by the accuracy of the algorithms used.^{5,6}

The pulse pressure waveform of an individual subject is known to contain vital information about the physical attributes and acts as an indicator of cardiovascular diseases.⁷ Pulse transit time (PTT) is known to be related to arterial stiffness, and it has also established its usefulness in the estimation of variation in systolic blood pressure.^{8,9} PTT is defined as the time duration for the pulse pressure waveform to propagate from the aortic valve to the peripheral site in an artery.¹⁰ Commonly, PTT is obtained from the “R” wave peak of an electrocardiogram (ECG) and the arrival of the pulse pressure at specific peripheral arterial site detected by photoplethysmogram (PPG).^{11,12} The main

disadvantage of this method is the time synchronization difficulty between the ECG and PPG. Some PPG devices induce undesired variable phase delay in the acquired signals, which will affect the PTT measurements.¹³

In the present study, the pulse transit time differential (PTTD) is measured from the pulse pressure waveform obtained at the carotid arterial site and radial arterial site using the fiber Bragg grating pulse recorder (FBGPR). FBGPR provides a noninvasive way of acquiring the pulse pressure waveform from the superficial impulses produced at the arterial site.^{14,15} PTTD is the time interval between the arrival of the pulse pressure waveform at the carotid arterial site and radial arterial site, which is essentially the difference in the PTT between the heart to the carotid arterial site and radial arterial site, respectively. Further, the measured PTTD is investigated for being an indicator from which the variation of systolic blood pressure may be derived, along the lines of the Moens–Korteweg’s equation.¹⁶ The evaluated variation in systolic blood pressure obtained from the PTTD is validated against the variation in the systolic blood pressure obtained from the Mindray Patient Monitor. Also, the pulse wave velocity computed from the obtained PTTD is validated against the pulse wave velocity measurements from the color Doppler ultrasound (CDU) technique, facilitating simultaneous data acquisition by both sensor methodologies. The present study reports a new methodology of acquiring the arterial pulse from the carotid and radial arterial sites using FBGPRs with which the novel parameter of PTTD can be evaluated. The proposed technique of PTTD measurement from FBGPR eliminates the use of two sensor methodologies

*Address all correspondence to: Sundarrajan Asokan, E-mail: sundarrajan.asokan@gmail.com

along with the time synchronization complexity, as data from both the FBGPRs at the carotid and radial arterial sites are acquired with a single time scale. In addition, the use of FBG sensor brings potential advantages such as insensitivity to electromagnetic interference, low fatigue, and ultrafast response, making the proposed FBGPR an effective means for PTTD measurement.

2 Materials and Methods

2.1 Theory of Fiber Bragg Grating

FBG is a periodic modulation of the refractive index of the core of a single-mode photosensitive optical fiber along its axis.¹⁷ When a broadband light is launched into an FBG, a single wavelength that satisfies the Bragg condition will be reflected back while the rest of the spectrum is transmitted.¹⁸ This reflected Bragg wavelength (λ_B) of the FBG is given by

$$\lambda_B = 2 n_{\text{eff}} \Lambda. \quad (1)$$

Here, Λ is the periodicity of the grating and n_{eff} is the effective refractive index of the fiber core.

Any external perturbation, such as strain, temperature, etc., at the grating site of the FBG sensor will alter the periodicity of the grating and, in turn, the reflected Bragg wavelength. By interrogating the shift in Bragg wavelength, the parametric external perturbation can be quantified.^{19–21} For example, the strain effect on an FBG sensor is expressed as

$$\Delta\lambda_B = \lambda_B \left\{ 1 - \frac{n_{\text{eff}}^2}{2} [P_{12} - \nu(P_{11} - P_{12})] \right\} \mathcal{E}, \quad (2)$$

where P_{11} and P_{12} are components of the strain-optic tensor, ν is the Poisson's ratio, and \mathcal{E} is the axial strain change.²² The strain sensitivity of an FBG inscribed in a germania-doped silica fiber is $\sim 1.20 \text{ pm}/\mu\mathcal{E}$.²³

In the present experiments, FBG sensors with a gauge length of 3 mm fabricated in a photosensitive Germania-doped silica fiber using the phase mask method²⁴ are employed. The temperature effect on the FBG sensor is neglected as the experiment is conducted in a controlled environment and the experimental duration is small.

2.2 Color Doppler Ultrasound Imaging

CDU instruments are real-time B-mode scanners with built-in Doppler capabilities. By estimating the mean Doppler shift caused by the blood flow velocity component of a vessel, CDU produces two-dimensional color-coded images of flow conditions superimposed on two-dimensional gray-scale images of anatomical structures.²⁵ CDU is capable of visualizing an artery with B-mode images of blood vessels and adjacent tissues in real time, along with the blood flow velocity component in the vessel.²⁶ This method is shown to be accurate and precise, hence making it a qualitative flow visualization tool.²⁷ In the present study, the Doppler shift component is utilized for measurement of blood flow velocity. Some of the drawbacks of CDU are dependency on skilled operator, instrument-dependent variables, computationally expensive, and burdensome for low-end ultrasound machines.^{28–30}

2.3 Principle of Estimation of Variation in Blood Pressure from PTTD

Dimensions and compliancy of the vessel are the primary parameters that influence the pulse wave velocity in the vessel. The Moens–Korteweg equation shows the relation between pulse wave velocity and the increasing elastic modulus of the arterial wall or its distensibility.³¹

$$v = \sqrt{\frac{gEa}{\rho d}}, \quad (3)$$

where v is the pulse wave velocity; g is the gravitational constant; E is the elastic modulus of the vessel; ρ is the density of the blood traveling within the vessel; a is the wall thickness; and d is the interior diameter of the vessel. An increase in blood pressure inside the vessel results in an increase in its diameter and decrease in its wall thickness and vice versa. Also, an increase in blood pressure inside the vessel results in an exponential increase of its elastic modulus,³² given by

$$E = E_0 e^{\gamma P}, \quad (4)$$

where E_0 is the elastic modulus at zero pressure; P is the blood pressure (mm Hg), and γ is a coefficient ranging from 0.016 to 0.018 (mm Hg^{-1}),^{10,16} depending on the particular vessel parameters. The change in elastic modulus of the vessel is much higher than the change in wall thickness and vessel diameter. Hence, it is observed that an increase in blood pressure induces an increase in pulse wave velocity.^{10,16} The pulse wave velocity is inversely proportional to the PTT and is given by

$$v = \frac{K}{\text{PTT}}, \quad (5)$$

where K is a distance between the two sensing points of the vessel (m) traveled by the pulse wave within time PTT (s) and the pulse wave velocity denoted by v (m/s). Combining Eqs. (3), (4), and (5), blood pressure can be expressed as^{10,16}

$$P = \frac{1}{\gamma} \left[\ln \left(\frac{\rho d K^2}{g a E_0} \right) - 2 \ln(\text{PTT}) \right]. \quad (6)$$

Assuming that the changes in dimensions of the vessel are negligible compared to the change in blood pressure and assuming that the change in the elastic modulus is slow enough, the variation in blood pressure for a short interval of time can be given by¹⁶

$$\Delta P = - \frac{2}{\gamma(\text{PTT})} \Delta \text{PTT}. \quad (7)$$

Equation (7) shows that for a short interval of time, with the assumption that variation in elastic modulus is slow, the variation in blood pressure varies linearly with the variation in PTT. It is important to note here from previous studies that this methodology is only comparable with the variation in systolic blood pressure and not the diastolic blood pressure.^{33–35}

In the present study, the measured PTTD (acquired from two different arteries), which is characteristically similar to PTT (acquired from two sites of the same artery), is investigated

for indicating the variation in systolic blood pressure and pulse wave velocity.

2.4 Experimental Methodology

The FBGPRs used in the present work are essentially a silicone diaphragm adhered onto a open bottom hollow box structure, along with an FBG sensor surface bonded by an industrial grade adhesive on the exterior surface of the silicone diaphragm as shown schematically in Fig. 1. The FBGPRs are positioned such that the silicon diaphragm facade consisting of an FBG sensor rests on the maximal impulse site of the arterial pressure pulse. The pulsatile flow of blood in the artery applies pressure on the silicone diaphragm and the strain variations generated as a consequence on the silicone diaphragm are sensed by the FBG sensor, which provide fundamental quantitative information of arterial pulse pressure waveform.^{14,15}

The experiments in the present study are within the guidelines of the institutional ethics for human studies and are carried

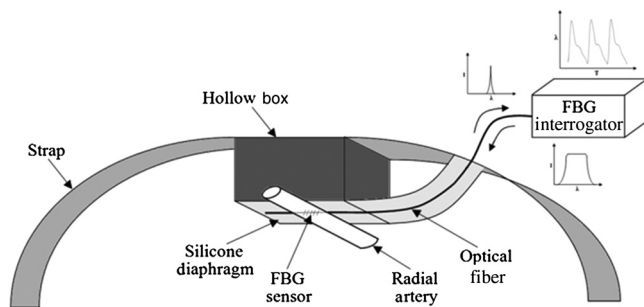


Fig. 1 Schematic representation of the fiber Bragg grating pulse recorder (FBGPR).¹⁴

out under the strict supervision of a registered medical practitioner. Also, the subjects have been fully informed about the experimental procedure and their consent is obtained prior to the experiments. Thirty subjects (18 male and 12 female) aged between 24 and 29 years, who are nonsmokers, nonalcoholic, nonhypertensive, and without any known cardiovascular diseases, have volunteered for the present study. Prior to the onset of the test, the subjects are made to sit comfortably on a chair with a back rest and are allowed to acclimatize to the surroundings for 15 min. A Riva Rocci cuff, which measures the blood pressure, is tied around the left arm and a finger pulse oximeter, which measures the heart rate, is clipped on the middle finger of the left arm, together with the Mindray Patient Monitor MEC 1200. Two FBGPRs connected via two separate fibers are employed in the present study to measure the pulse pressure waveform at the carotid arterial site (reflected center Bragg wavelength of 1546 nm) and radial arterial site of the right hand (reflected center Bragg wavelength of 1530 nm) simultaneously. The reflected Bragg wavelengths from both the FBGPRs are acquired using a Micron Optics SM 130-700 interrogator whose reflected spectrum is shown in Fig. 2, with a sampling frequency of 1 kHz or at the rate of one sample per millisecond.

The CDU probe (Siemens Acuson S2000) is also placed over the right wrist of the test arm proximal to the FBGPR to measure the pulse wave velocity in the radial artery as shown in Fig. 3. The test duration is 10 min during which the arterial pulse waveforms from both FBGPRs at the carotid and radial arterial sites are continuously recorded. Simultaneously, the blood pressure readings are obtained from the Mindray Patient Monitor with a time interval of 1 min and the pulse wave velocity from CDU technique is obtained once midway during the experiment.

The PTTD is computed as the time interval between the peak pulse pressures at both the carotid and radial arterial sites. By

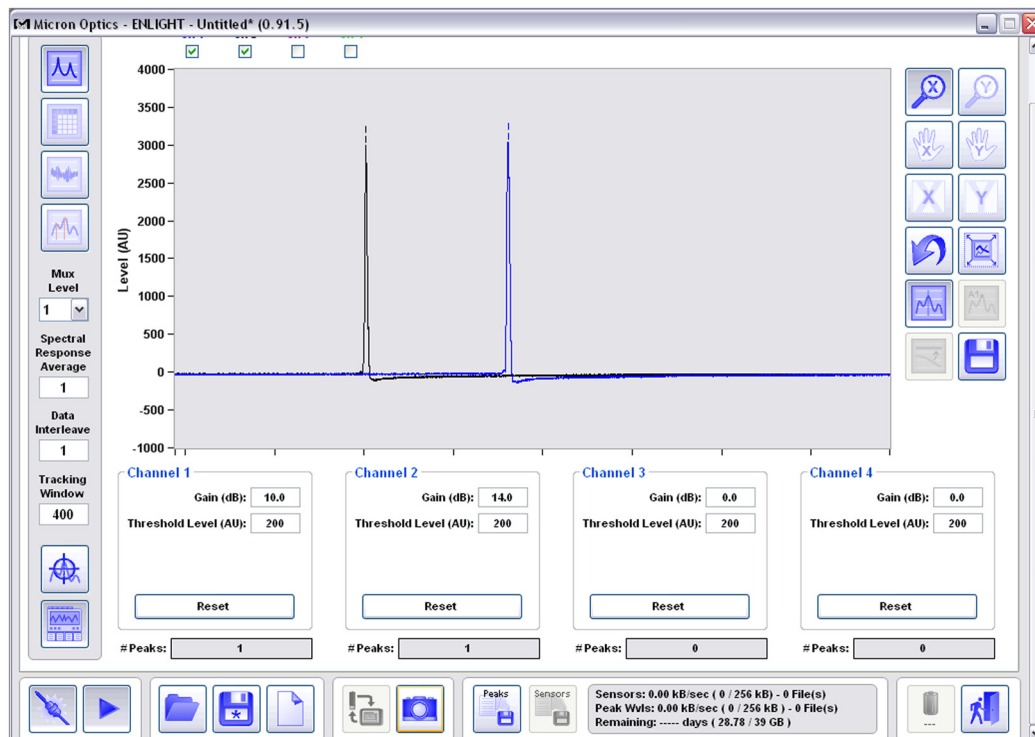


Fig. 2 Reflection spectrum obtained from FBG sensors employed in the two FBGPRs.



Fig. 3 Simultaneous data acquisition from FBGPRs, color Doppler ultrasound (CDU), and Mindray Patient Monitor during the experimental test.

measuring the extra path traveled (P_3) by the pulse pressure wave sensed at the radial arterial site (one arm length as shown in Fig. 4), compared to the carotid arterial site, the pulse wave velocity in the radial artery is estimated from the PTTD using Eq. (5). This is carried out with an assumption that the path length and pulse wave velocity are almost similar in both paths P_1 and P_2 . This assumption is considered on the basis that the superficial lengths of P_1 and P_2 are almost similar. Also, as the blood is being pumped from the brachiocephalic trunk to both the carotid artery and radial artery, the pulse wave velocity is assumed to be identical. Further, the variation in the systolic blood pressure is evaluated from the variation in the PTTD using Eq. (7).

3 Results and Discussion

The data obtained from a typical male of age 25 years is selected for illustration. The pulse pressure waveforms from both the carotid and radial arterial site are obtained simultaneously and are compared against time as shown in Fig. 5. The PTTD computed between three consecutive heart beats are 0.918, 0.924, and 0.903 s for the illustrated subject, respectively, as depicted in Fig. 5. The resolution of the PTTD measurement is one millisecond, as per the ability of the data acquisition system. Also, the time duration between consecutive peak pulse pressures from both the carotid and radial arterial sites (0.95 and 0.97 s) are compared for identification of corresponding pulses generated from the same heart beat obtained at both sites. It is also observed that the pulse pressure waveform pattern obtained from both carotid and radial arterial sites are characteristically similar to the pulse pressure waveform pattern obtained at the

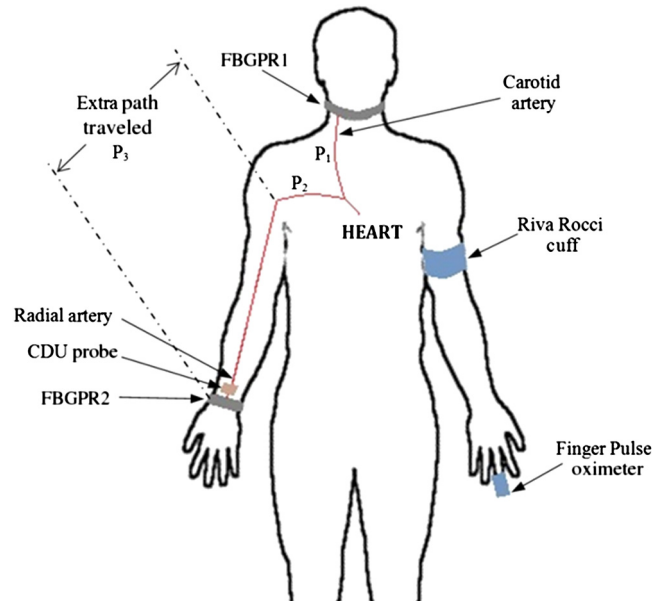


Fig. 4 The schematic of the positions of FBGPRs, CDU, and Mindray Patient Monitor, along with the depiction of the extra path of travel.

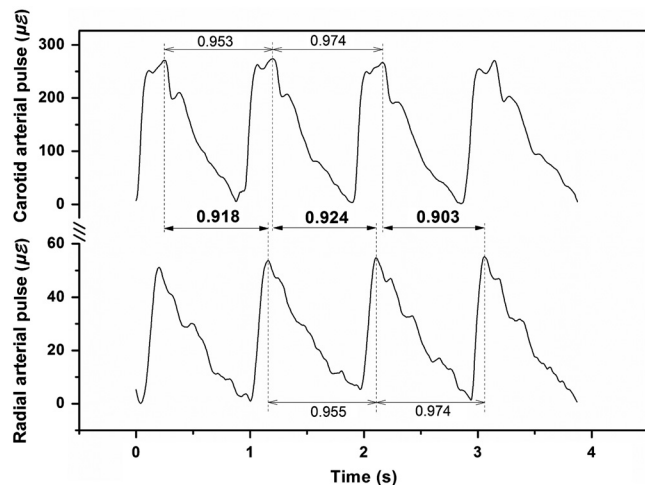


Fig. 5 Pulse pressure waveform obtained at carotid and radial arterial sites compared with respect to time.

respective sites from previous studies.^{36–38} Simultaneously, the systolic blood pressure in the radial artery is acquired from the Mindray Patient Monitor and the pulse wave velocity from CDU.

For the illustrated subject, the average value of PTTD obtained is 0.915 s. The pulse wave velocity obtained from the CDU at the radial artery is 46.1 cm/s as shown in Fig. 6. The extra path traveled by the pulse pressure wave, which is one arm length of the subject, is measured to be 41.5 cm. From Eq. (5), the pulse wave velocity estimated from the FBGPRs is 45.35 cm/s, which is in good agreement with the pulse wave velocity obtained from CDU. Also, from Eq. (7), the variation in systolic blood pressure is estimated from the recorded PTTD and is compared with the variation in systolic blood pressure obtained from the Mindray Patient Monitor as shown in Fig. 7. A correlation coefficient of 0.84 is observed between the variations of systolic blood pressure by both methodologies, demonstrating the agreement of their results.

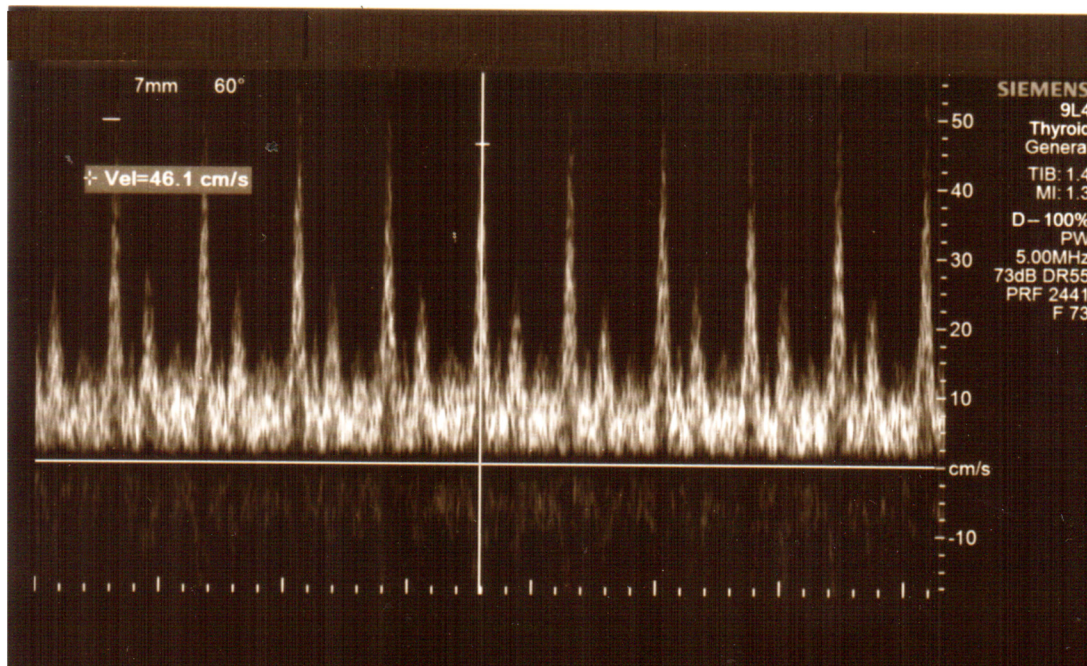


Fig. 6 Pulse wave velocity measurement from CDU.

Similar tests are carried out on all 30 subjects. An average PTTD during the test time of 10 min is calculated and the corresponding pulse wave velocities for all individual subjects are estimated. The pulse wave velocity determined from the PTTD and pulse wave velocity from the CDU of all the 30 subjects are compared with each other as shown in Fig. 8. A correlation coefficient of 0.89 is observed between them, which signifies that the pulse velocities obtained from both the methodologies are in good accordance.

As illustrated, the variation of systolic blood pressure from the FBGPRs and Mindray Patient Monitor is compared individually for all 30 subjects and the obtained correlation coefficients are shown in Table 1. It is observed that the correlation coefficients obtained range from 0.57 to 0.93, with the mean

correlation coefficient for all subjects being 0.78. The moderate value of 0.78 obtained for the mean correlation coefficient shows that the variation in PTTD operates as an indicator of variation in systolic blood pressure. The variation in the correlation coefficients obtained among subjects can be largely attributed to the accuracy of blood pressure measurements obtained from the Mindray Patient Monitor by the oscillometric technique.

The present study reports a new methodology of acquiring the arterial pulse pressure from the carotid and radial arterial sites using FBGPRs. From the time interval between the peak pulse pressures obtained at carotid and radial arterial sites, the novel parameter of PTTD is evaluated. By the compilation of all the results obtained, it can be observed that the PTTD is similar to PTT in the aspect of functioning as an indicator of variation of systolic blood pressure and pulse wave velocity. Furthermore,

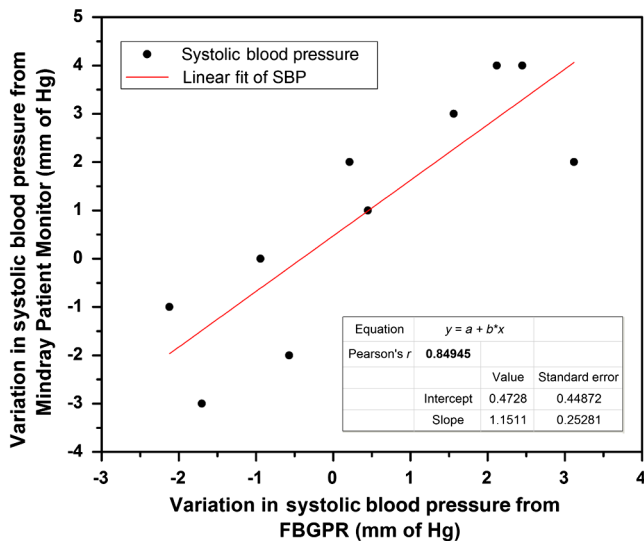


Fig. 7 Comparison of variations in systolic blood pressure obtained from FBGPRs and Mindray Patient Monitor.

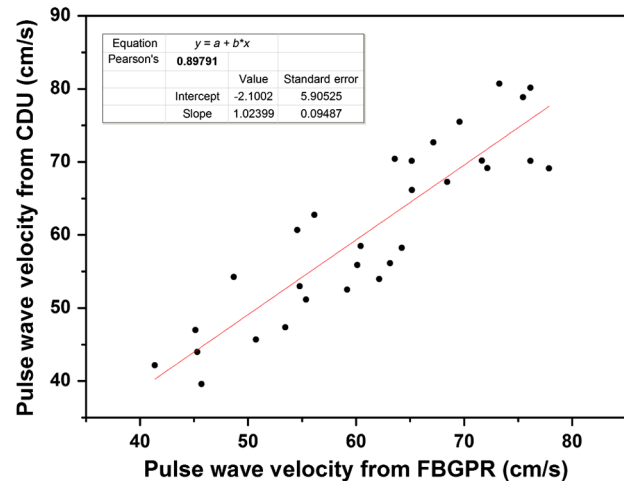


Fig. 8 Comparison of pulse wave velocities from FBGPRs and CDU for all the subjects.

Table 1 Correlation coefficients of all subjects, evaluated by comparison of variation in systolic blood pressures obtained from fiber Bragg grating pulse recorders and Mindray Patient Monitor.

Subject	Correlation coefficient (r)	Subject	Correlation coefficient (r)	Subject	Correlation coefficient (r)
Sub 1	0.84	Sub 11	0.65	Sub 21	0.88
Sub 2	0.78	Sub 12	0.77	Sub 22	0.78
Sub 3	0.86	Sub 13	0.73	Sub 23	0.61
Sub 4	0.91	Sub 14	0.86	Sub 24	0.83
Sub 5	0.71	Sub 15	0.57	Sub 25	0.88
Sub 6	0.68	Sub 16	0.75	Sub 26	0.79
Sub 7	0.89	Sub 17	0.93	Sub 27	0.80
Sub 8	0.87	Sub 18	0.82	Sub 28	0.83
Sub 9	0.92	Sub 19	0.74	Sub 29	0.76
Sub 10	0.61	Sub 20	0.68	Sub 30	0.70

Mean: 0.781 Standard deviation: 0.098 Range: 0.57 to 0.93

any positional offset of the FBGPR over the artery or variation in applied pressure on the artery by the FBGPR is of no consequence, as the PTTD measurements are time based and not strain amplitude based.

4 Conclusion

The present study proposes a novel noninvasive methodology to measure the PTTD by acquiring the pressure pulse waveform at the carotid and radial arterial sites with the aid of FBGPRs. The measured PTTD is found to be characteristically similar to pulse transit time. The beat-to-beat variation of systolic blood pressure and pulse wave velocity is derived from the measured PTTD. A major advantage of the present technique of PTTD measurement from FBGPR is the elimination of the use of two sensor methodologies. This reduces the time synchronization complexity, as the data from both the FBGPRs are acquired simultaneously on a single time scale. A test bench is currently under development to experimentally characterize the measurement errors during estimation of pulse wave velocity and variation of systolic blood pressure, along with the acceptable range of PTTD measurements by the FBGPRs methodology with a substantial sample size. Further, this study can be extended to subjects of varying age categories and persistent cardiovascular problems.

Acknowledgments

The partial financial support of Robert Bosch Centre for Cyber Physical Systems, Indian Institute of Science, is gratefully acknowledged.

References

- W. C. Cushman, "The burden of uncontrolled hypertension: morbidity and mortality associated with disease progression," *J. Clin. Hypertens.* **5**(3), 14–22 (2003).
- M. Ward and J. A. Langton, "Blood pressure measurement," *Contin. Educ. Anaesth. Crit. Care Pain.* **7**(4), 122–126 (2007).
- D. Perloff et al., "Human blood pressure determination by sphygmomanometry," *Circulation* **88**, 2460–2470 (1993).
- N. R. Campbell et al., "Accurate, reproducible measurement of blood pressure," *Can. Med. Assoc. J.* **143**(1), 19–24 (1990).
- T. G. Pickering et al., "Blood pressure measurement in humans," *Hypertension* **45**, 142–161 (2005).
- J. Penaz, "Photoelectric measurement of blood pressure, volume and flow in the finger," in *Digest of the 10th Int. Conf. on Medical and Biological Engineering*, p. 104 (1973).
- Y. Choi, Q. Zhang, and S. Ko, "Noninvasive cuffless blood pressure estimation using pulse transit time and Hilbert–Huang transform," *Comput. Electr. Eng.* **39**, 103–111 (2013).
- P. Lantelme et al., "Heart rate: an important confounder of pulse wave velocity assessment," *Hypertension* **39**, 1083–1087 (2002).
- J. Y. Foo and C. S. Lim, "Pulse transit time as an indirect marker for variations in cardiovascular related reactivity," *Technol. Health Care* **14**(2), 97–108 (2006).
- C. Ahlstrom et al., "Noninvasive investigation of blood pressure changes using the pulse wave transit time: a novel approach in the monitoring of hemodialysis patients," *J. Artif. Organs* **8**, 192–197 (2005).
- R. P. Smith et al., "Pulse transit time: an appraisal of potential clinical applications," *Thorax* **54**, 452–457 (1999).
- J. Allen, "Photoplethysmography and its application in clinical physiological measurement," *Physiol. Meas.* **28**, R1–R39 (2007).
- J. Y. A. Foo et al., "Variability in time delay between two models of pulse oximeters for deriving the photoplethysmographic signals," *Physiol. Meas.* **26**, 531–544 (2005b).
- U. Sharath et al., "Blood pressure evaluation using sphygmomanometry assisted by arterial pulse waveform detection by fiber Bragg grating pulse device," *J. Biomed. Opt.* **18**(6), 067010 (2013).
- U. Sharath et al., "Radial arterial compliance measurement by fiber Bragg grating pulse recorder," *J. Hum. Hypertens.* **28**, 736–742 (2014).
- W. Chen et al., "Continuous estimation of systolic blood pressure using the pulse arrival time and intermittent calibration," *Med. Biol. Eng. Comput.* **38**, 569–574 (2000).
- W. W. Morey, G. Meltz, and W. H. Glenn, "Fiber Bragg grating sensors," *Proc. SPIE* **1169**, 98–107 (1989).
- A. Othonos, "Fiber Bragg gratings," *Rev. Sci. Instrum.* **68**(12), 4309–4341 (1997).
- A. D. Kersey et al., "Fiber grating sensors," *J. Lightwave Technol.* **15**, 1442–1462 (1997).
- A. Othonos and K. Kalli, *Fiber Bragg Gratings: Fundamentals and Applications in Telecommunications and Sensing*, Artech House, Boston (1999).
- R. Kashyap, *Fiber Bragg Gratings*, Academic Press, San Diego (1999).
- B. A. Tahir, J. Ali, and R. A. Rahman, "Fabrication of fiber grating by phase mask and its sensing application," *J. Optoelectron. Adv. Mater.* **8**(4), 1604–1609 (2006).
- S. M. Melle et al., "A Bragg grating-tuned fibre laser strain sensor system," *IEEE Photon. Technol. Lett.* **5**, 263–266 (1993).
- K. O. Hill et al., "Bragg gratings fabricated in monomode photosensitive optical fiber by UV exposure thorough a phase-mask," *Appl. Phys. Lett.* **62**, 1035–1037 (1993).
- H. Sava et al., "A 3D colour Doppler ultrasound imaging system for in vitro estimation of flow parameters downstream of prosthetic heart valves," in *Proc. of the 20th Annual Int. Conf. of the IEEE Engineering in Medicine and Biology Society*, Vol. **2**, pp. 800–803 (1998).
- C. Kasai et al., "Real-time two-dimensional blood flow imaging using an autocorrelation technique," *IEEE Trans. Sonics Ultrason.* **32**, 458–464 (1985).
- D. W. Rickey, R. Rankin, and A. Fenster, "A velocity evaluation phantom for colour and pulsed Doppler instruments," *Ultrasound Med. Biol.* **18**(5), 479–494 (1992).
- P. A. Picot et al., "Rapid volume flow rate estimation using transverse colour Doppler imaging," *Ultrasound Med. Biol.* **21**(9), 1199–1209 (1995).
- D. G. Mitchell, "Colour Doppler imaging: principles, limitations and artefacts," *Radiology* **177**, 1–10 (1990).

30. T. Fukuoka et al., "Ultrasound color Doppler imaging on a fully programmable architecture," in *IEEE Ultrasonics Symp.*, pp. 1639–1642 (2006).
31. J. W. Remington, "The physiology of the aorta and major arteries," Chapter 24 in *Handbook of Physiology*, W. F. Hamilton and P. Dow, Eds., pp. 799–838, American Physiological Society, Washington, D.C. (1963).
32. D. J. Hughes et al., "Measurement of Young's modulus of elasticity of the canine aorta with ultrasound," *Ultrason. Imaging* **1**, 356–367 (1979).
33. R. Ochiai et al., "The relationship between modified pulse wave transit time and cardiovascular changes in isoflurane anesthetized dogs," *J. Clin. Monit. Comput.* **15**, 493–501 (1999).
34. R. A. Payne et al., "Pulse transit time measured from the ECG: an unreliable marker of beat-to-beat blood pressure," *J. Appl. Physiol.* **100**, 136–141 (2006).
35. J. Y. A. Foo, "A computational approach to predict pulse transit time variations during postural change," *Cardiovasc. Eng.* **7**, 121–126 (2007).
36. S. J. Vermeersch et al., "Determining carotid artery pressure from scaled diameter waveforms: comparison and validation of calibration techniques in 2026 subjects," *Physiol. Meas.* **29**(11), 1267–1280 (2008).
37. Y. K. Yim et al., "Gender and measuring-position differences in the radial pulse of healthy individuals," *J. Acupunct. Meridian Stud.* **7**(6), 324–330 (2014).
38. C. Leitão et al., "Feasibility studies of Bragg probe for noninvasive carotid pulse waveform assessment," *J. Biomed. Opt.* **18**(1), 017006 (2013).

Biographies of the authors are not available.